

## Supporting Information for

Controllable assembly of single/double-thin-shell g-C<sub>3</sub>N<sub>4</sub> vesicles via a shape-selective solid-state templating method for efficient photocatalysis

*Lei Luo*<sup>1, 2</sup>, *Keyan Li*<sup>1</sup>, *Anfeng Zhang*<sup>1</sup>, *Hainan Shi*<sup>1</sup>, *Guanghui Zhang*<sup>1</sup>, *Jiani Ma*<sup>2</sup>, *Wen Zhang*<sup>2</sup>,  
*Junwang Tang*<sup>2, 3\*</sup>, *Chunshan Song*<sup>1, 4\*</sup>, *Xinwen Guo*<sup>1\*</sup>

<sup>1</sup> State Key Laboratory of Fine Chemicals, PSU-DUT Joint Center for Energy Research, School of Chemical Engineering, Dalian University of Technology, Dalian 116024, P. R. China.

<sup>2</sup> Key Lab of Synthetic and Natural Functional Molecule Chemistry of Ministry of Education, and the Energy and Catalysis Hub, College of Chemistry and Materials Science, Northwest University, Xi'an 710069, P. R. China

<sup>3</sup> Department of Chemical Engineering, University College London, Torrington Place, London WC1E 7JE, UK.

<sup>4</sup> EMS Energy Institute, PSU-DUT Joint Center for Energy Research and Department of Energy & Mineral Engineering, Pennsylvania State University, University Park, Pennsylvania 16802, United States.

**\*Corresponding author 1: Xinwen Guo**

E-mail: guoxw@dlut.edu.cn

**\*Corresponding author 2: Chunshan Song**

E-mail: csong@psu.edu

**\*Corresponding author 3: Junwang Tang**

E-mail: junwang.tang@ucl.ac.uk

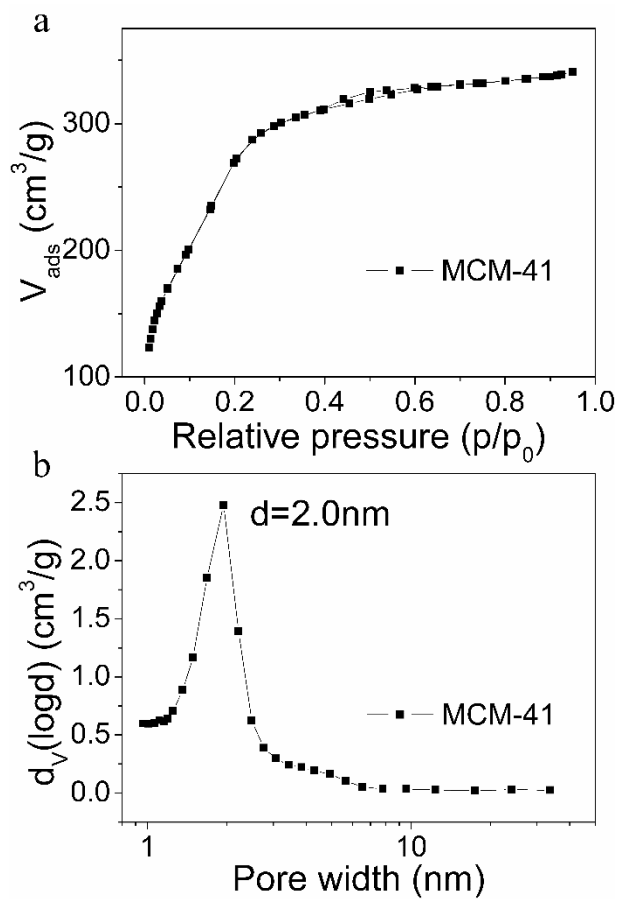


Figure S1. (a)  $N_2$  physical adsorption-desorption isotherms at 77 K and (b) the pore size distribution of MCM-41 calculated by BJH method.

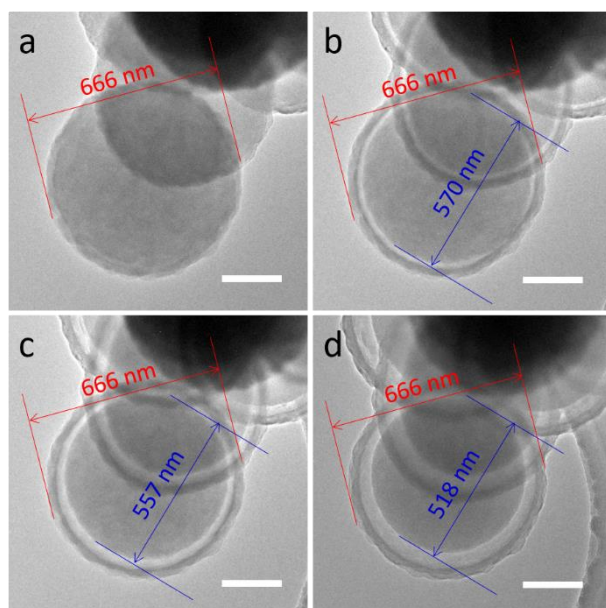


Figure S2. The TEM images of the identical MCM-41@g-C<sub>3</sub>N<sub>4</sub> nanoparticle at different electron beam radiation time. The radiation time is gradually extended from a to d. The scale bar is 200 nm.

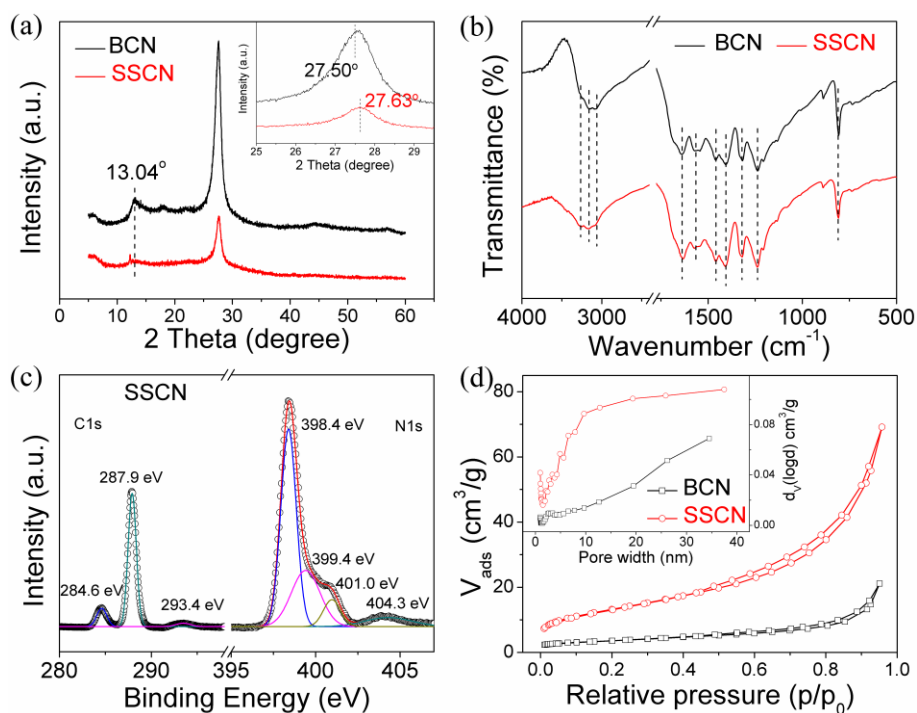


Figure S3. Structure and phase identification of BCN and SSCN. (a) XRD patterns, (b) FT-IR spectra, (c) C1s and N1s high resolution XPS spectra, (d) N<sub>2</sub> physical adsorption-desorption isotherms at 77K and the pore size distribution calculated by BJH method (shown inset).

Fourier transform-infrared (FT-IR) spectra are shown in Figure S3b and demonstrate the typical structure of g-C<sub>3</sub>N<sub>4</sub>. Series of strong bands at 1200-1600 cm<sup>-1</sup> and a sharp band at 810 cm<sup>-1</sup> were attributed to the stretching vibration and breathing mode of the heptazine heterocycle ring (C<sub>6</sub>N<sub>7</sub>) units of g-C<sub>3</sub>N<sub>4</sub>. The broad bands at 3000-3600 cm<sup>-1</sup> are assigned to the N-H and O-H bands, indicating the existence of the uncondensed amino groups and the absorbed water molecular on the surface of the as-prepared g-C<sub>3</sub>N<sub>4</sub>. Elemental analysis suggests all the three samples composed of carbon and nitride with a C/N molar ratio at ca. 0.67, which is lower than the ideal g-C<sub>3</sub>N<sub>4</sub> composition (C/N=0.75) because of the terminal uncondensed amino groups. X-ray photoelectric spectra (XPS) were conducted to further reveal the chemical composition (Figure S3c). Only three elements (C, N, O) were detected according to the survey XPS spectra. The O1s peak may be

attributed to the surface absorbed oxygen species[40], as confirmed by the FT-IR spectra. The two samples exhibit C1s and N1s signals with a surface C/N ratio at 0.76 and 0.81, close to the ideal g-C<sub>3</sub>N<sub>4</sub> composition. Furthermore, the absence of Si signal indicates that the silica templates were totally eliminated with the NH<sub>4</sub>HF<sub>2</sub> solution. The high resolution XPS spectra were conducted to further investigate the chemical state of carbon and nitride elements. In the case of the C1s spectra, two distinguished peaks were presented. The smaller peak at 284.6 eV is attributed to the sp<sup>2</sup> C-C bonds and usually used to normalize the XPS spectra. The other prominent peak at 287.9 eV is attributed to the N-C=N bonds in the heptazine heterocycle ring (C<sub>6</sub>N<sub>7</sub>) units. It is obvious that the latter carbon species is considered as the main carbon species in the g-C<sub>3</sub>N<sub>4</sub>. The N1s spectra were deconvoluted into four individual peaks at 398.4, 399.3, 401.0 and 404.0 eV, which are assigned to the C-N=C in the triazine ring, the tertiary nitrogen (N-(C)<sub>3</sub>), the terminal amino groups (-NH<sub>2</sub>) and  $\pi$ -excitations, respectively. The above results confirmed the essentially unchanged elemental state and content of g-C<sub>3</sub>N<sub>4</sub> under different synthetic conditions.

Nitrogen physical adsorption test at -196 °C were conducted to further characterize the textural properties of the as-prepared morphological g-C<sub>3</sub>N<sub>4</sub> and shown in Figure S3d and Table S1. As shown in Figure S3d, BCN exhibits type II adsorption isotherm, with a low surface area at 12.8 m<sup>2</sup>/g, which is in accordance with the literatures [41, 42]. As a comparison, the single-shelled g-C<sub>3</sub>N<sub>4</sub> presents an improved surface area of 48.0 m<sup>2</sup>/g, as shown in Table S1. Meanwhile, the H3 hysteresis loop indicates that SSCN was composed of fragmental g-C<sub>3</sub>N<sub>4</sub> nanosheets, but not a complete ink-bottle structure. Notably, the reason why the hollow structure evidenced by the SEM and TEM was not shown in the nitrogen physical sorption is attributed to the large pore size distribution (> 4 nm) of the shells, which results in the unclosed system of the as-prepared hollow structure.

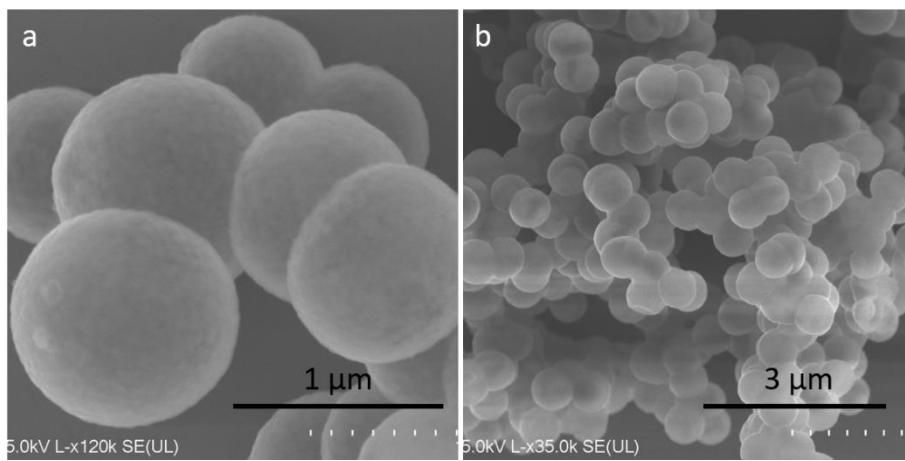


Figure S4. (a, b) SEM images of SSCN.

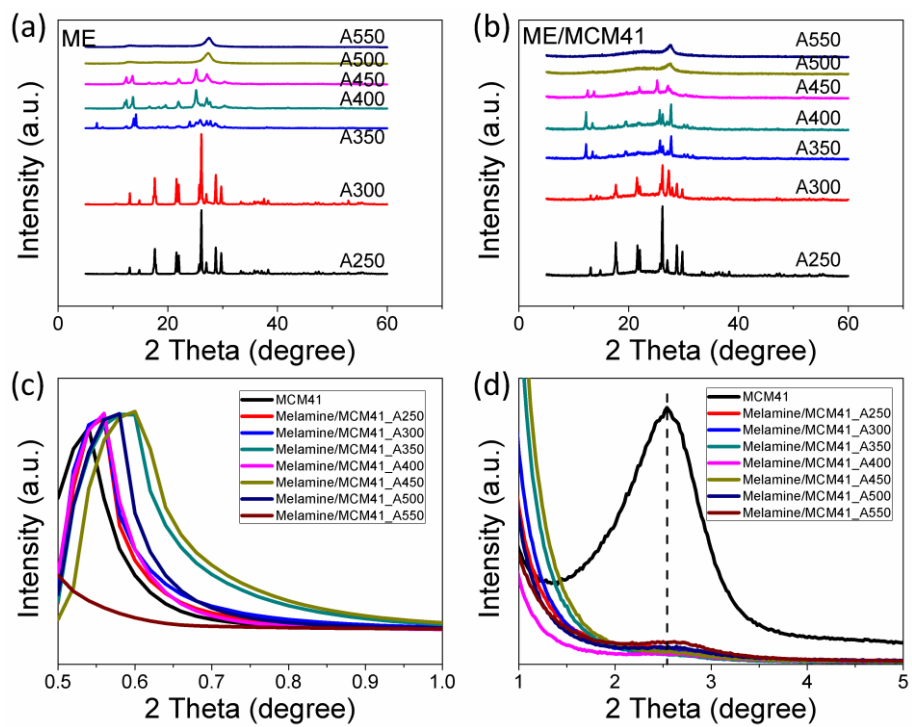


Figure S5. XRD patterns of  $g\text{-C}_3\text{N}_4/\text{MCM-41}$  composites prepared under different temperatures.

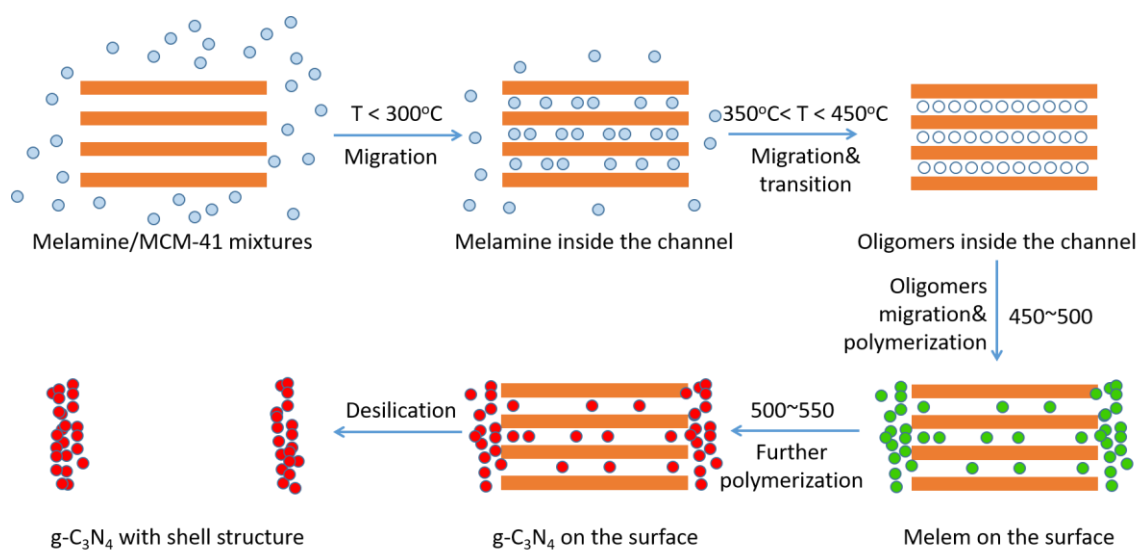


Figure S6. The schematic illustration of the migration and polymerization of the carbon and nitrogen species in the presence of MCM-41.

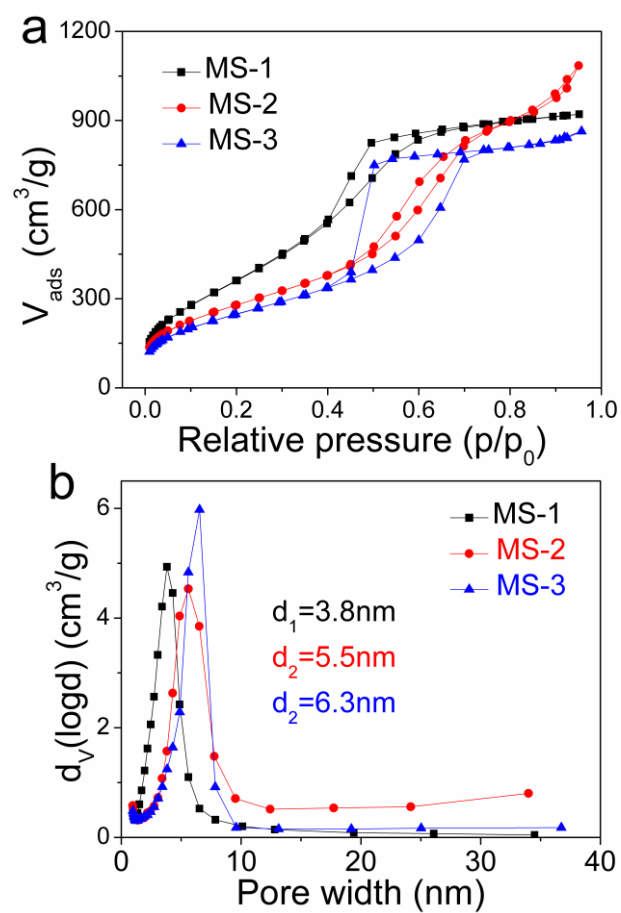


Figure S7. (a) Nitrogen physical adsorption-desorption isotherms and (b) the pore size distribution of series of MS-x silica. The pore size distribution is calculated by the BJH method.

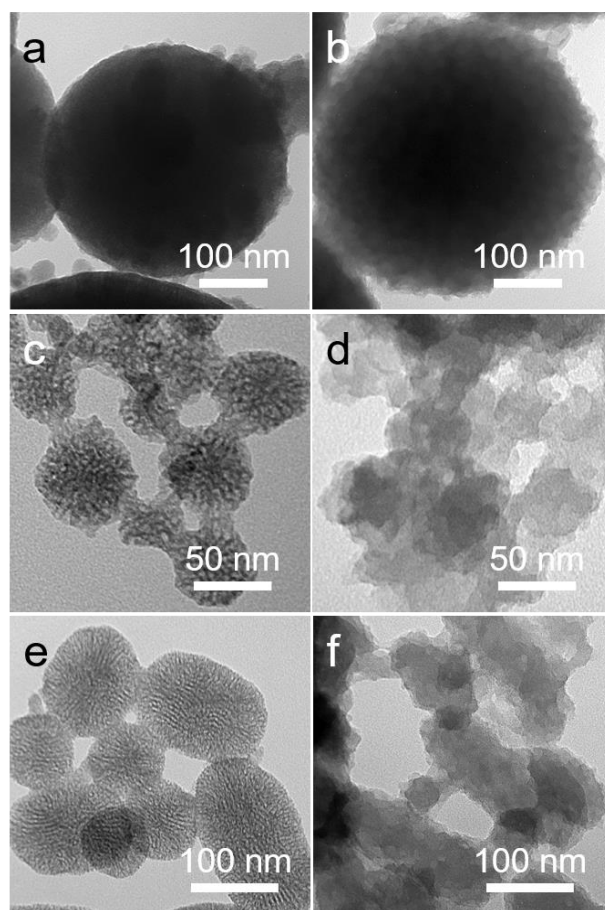


Figure S8. TEM images of (a, c, e) MS-1, MS-2 and MS-3, and (b, d, f) the as-templated g-C<sub>3</sub>N<sub>4</sub>.

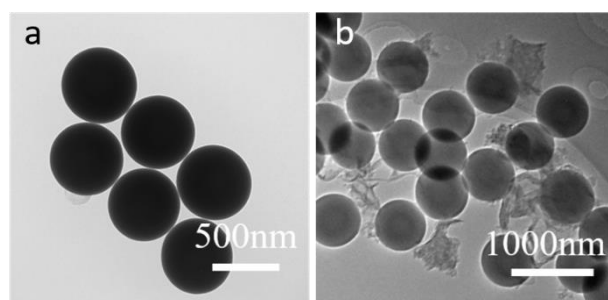


Figure S9. TEM images of (a) dense silica nanoparticles, (b) the products obtained from calcination of the mixtures of dense silica and melamine.

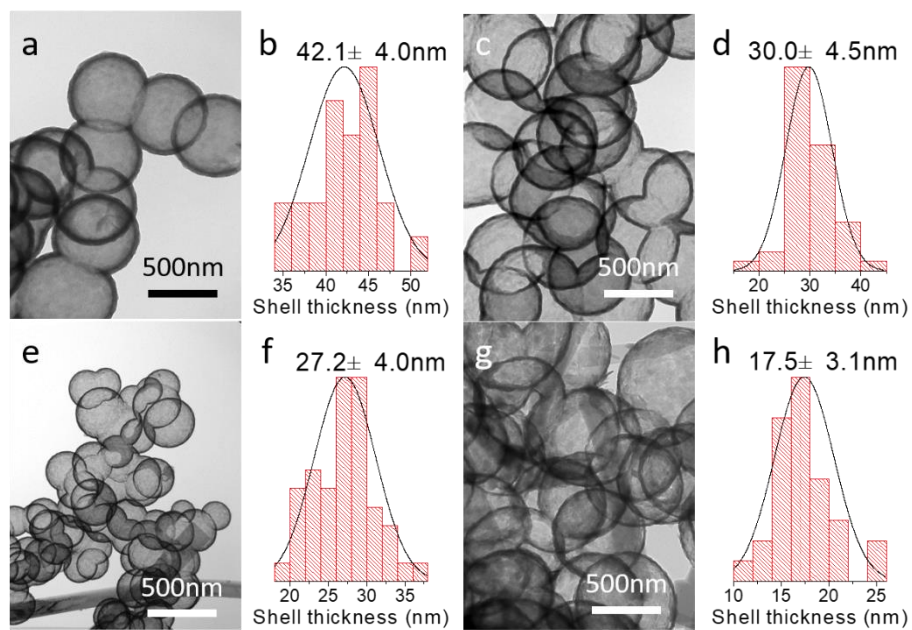


Figure S10. Single-shelled  $g\text{-C}_3\text{N}_4$  vesicles prepared with different mass ratio of melamine/MCM-

41. The ratio is (a) 0.1, (d) 0.3, (e) 0.5, (g) 0.8.

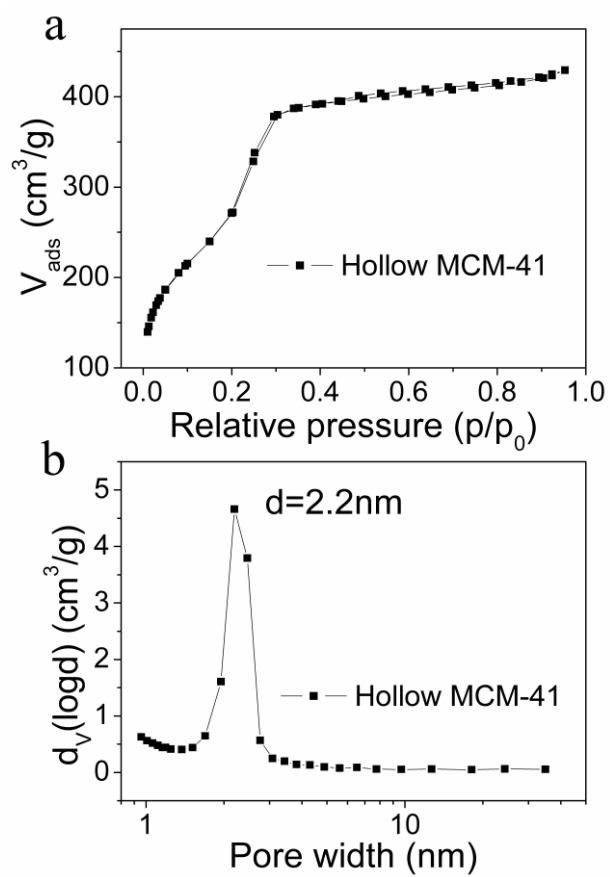


Figure S11. (a)  $N_2$  physical adsorption-desorption isotherms at 77 K and (b) the pore size distribution of hollow MCM-41 calculated by BJH method.

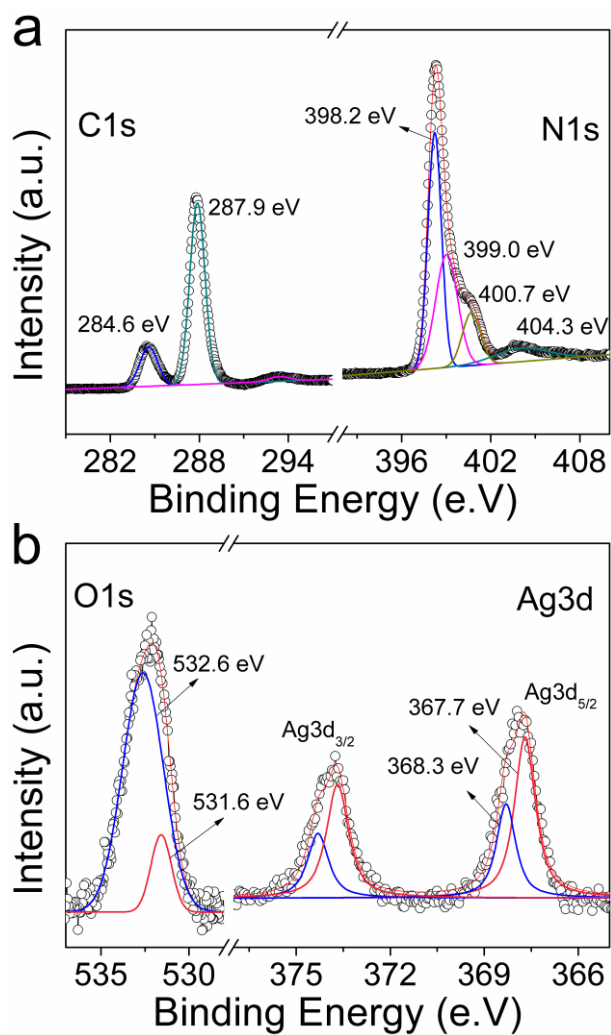


Figure S12. XPS spectra of Ag@SSCN: (a) C1s and N1s, (b) O1s and Ag3d.

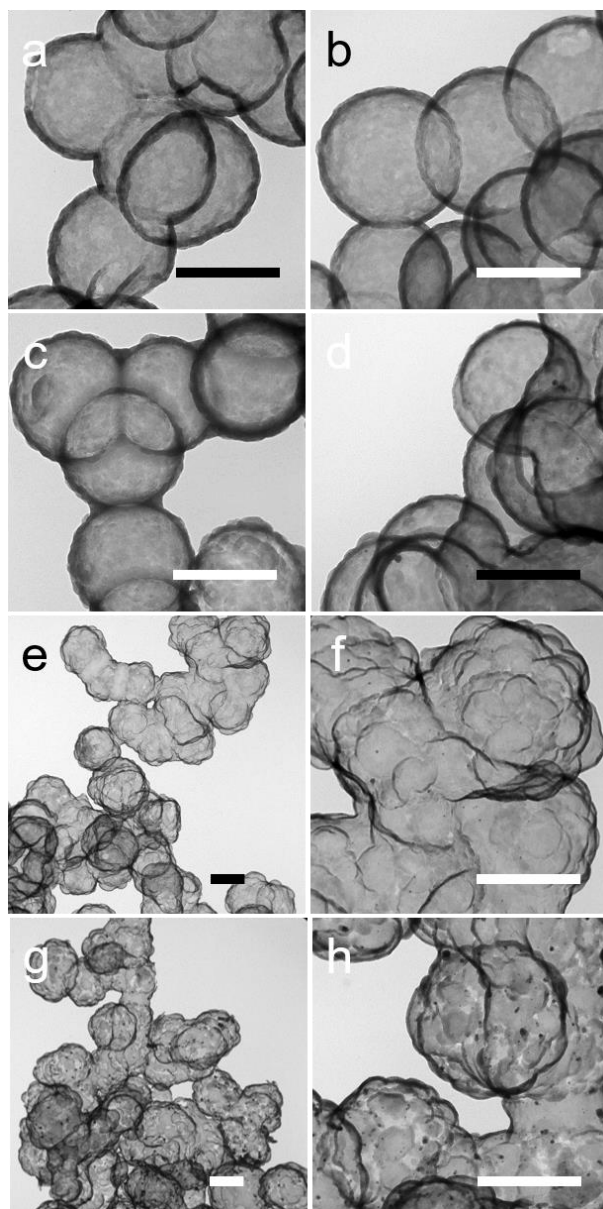


Figure S13. TEM images of (a) 0.3Ag@SSCN, (b) 1Ag@SSCN, (c) 3Ag@SSCN, (d) 6Ag@SSCN, (e, f) 10Ag@SSCN, (g, h) 15Ag@SSCN. The scale bar is 500 nm. The number in the sample code represents the mass ratio of silver in the template.

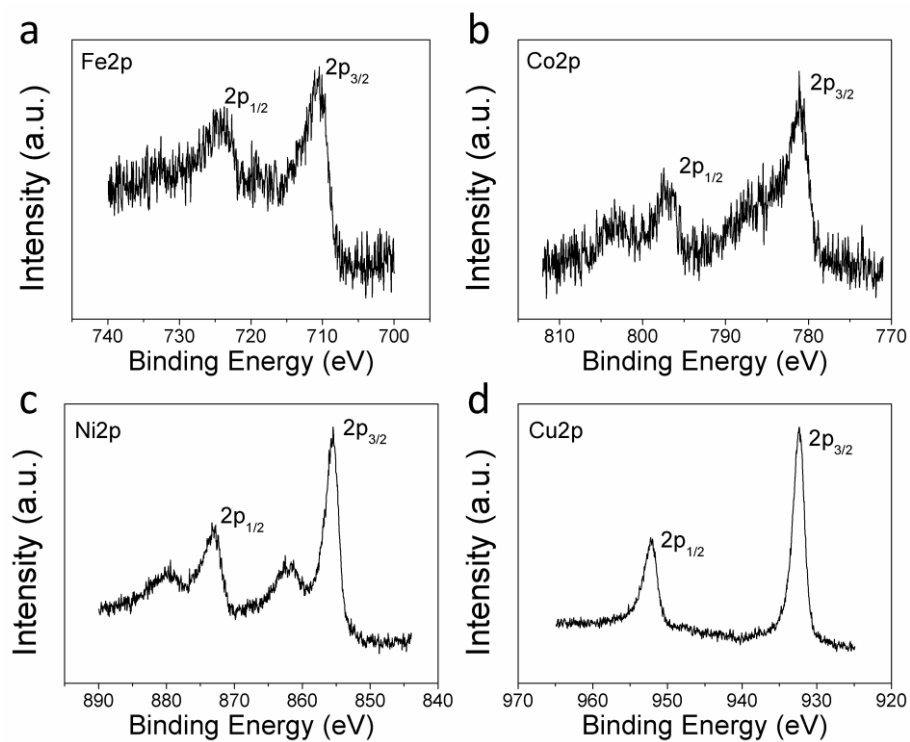


Figure S14. XPS spectra of (a) 3Fe@SSCN, (b) 3Co@SSCN, (c) 3Ni@SSCN and (d) 3Fe@SSCN.

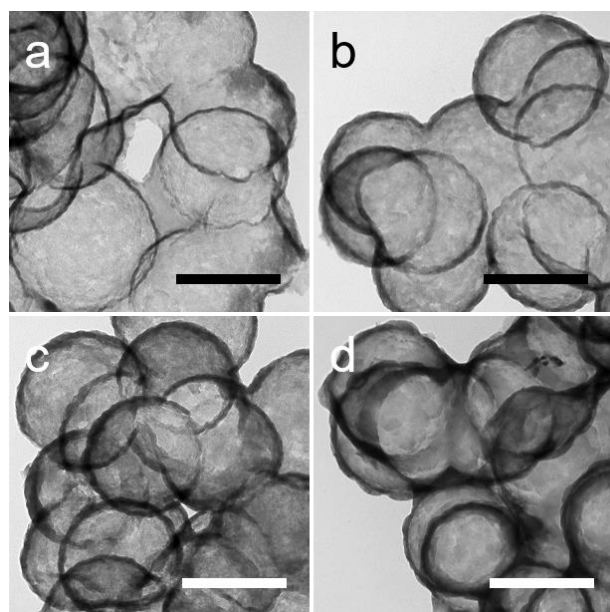


Figure S15. TEM images of (a) 3Fe@SSCN, (b) 3Co@SSCN, (c) 3Ni@SSCN and (d) 3Fe@SSCN.

The scale bar is 500 nm.

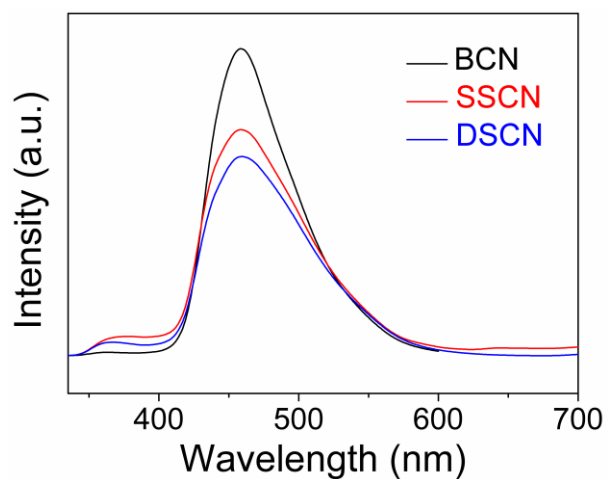


Figure S16. Steady-state photofluorescence spectra of BCN, SSCN and DSCN.

The steady-state photofluorescence (PL) spectra were performed to characterize the photogenerated charge carrier recombination efficiency. As shown in Figure S16, compared with the bulk  $g\text{-C}_3\text{N}_4$ , the morphological  $g\text{-C}_3\text{N}_4$  showed a consecutively weakened PL intensity from SSCN to DSCN. The most weakened PL intensity for DSCN indicates the lowest charge recombination efficiency, which is favorable to the photocatalysis.

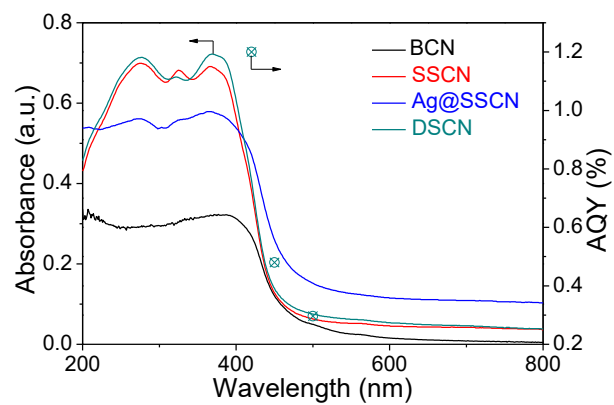


Figure S17. Wavelength dependent AQY and UV-DSR spectra of BCN, SSCN, Ag@SSCN and DSCN.

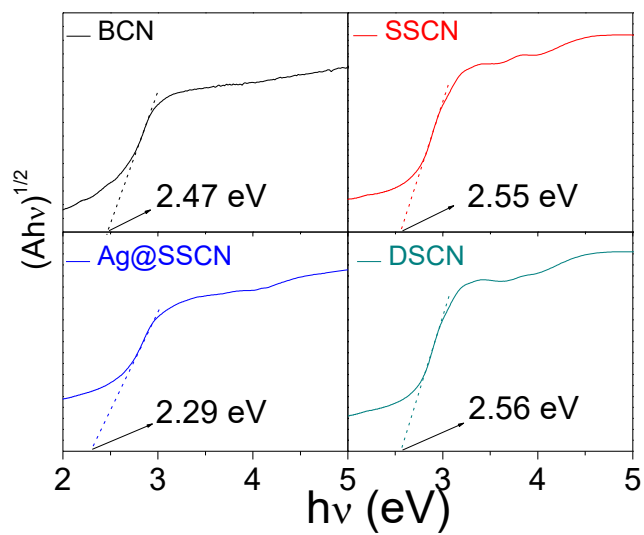


Figure S18. Tauc plots of BCN, SSCN, Ag@SSCN and DSCN.

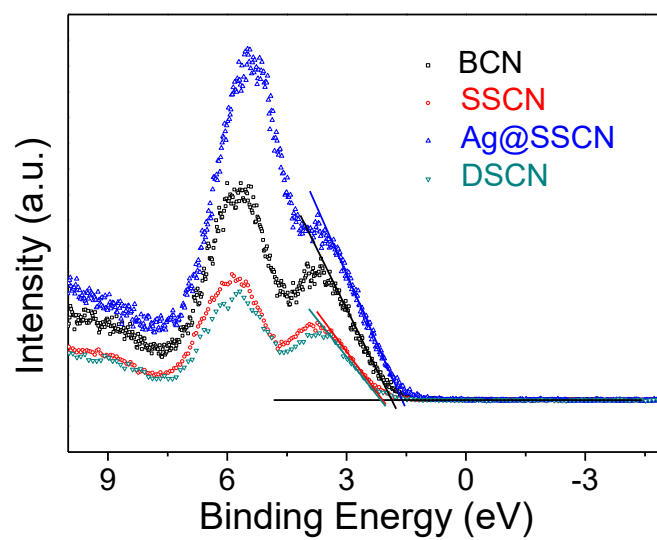


Figure S19. XPS-VB spectra of BCN, SSCN, Ag@SSCN and DSCN.

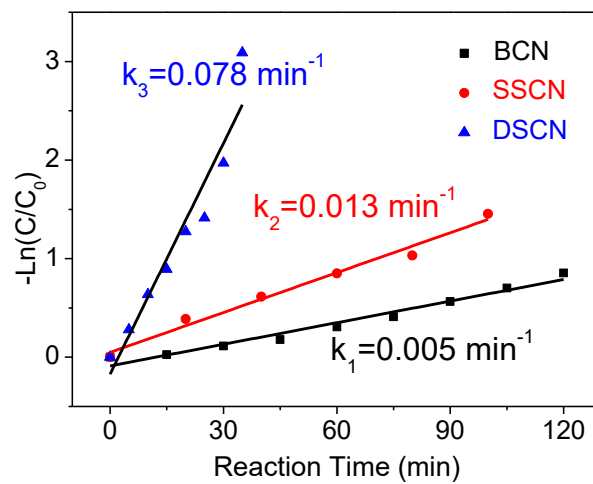


Figure S20. The first-order kinetic constant as a function of the reaction time.

Table S1. Textual properties and elemental composition of samples BCN, SSCN and DSCN.

| Sample | C/N <sup>1</sup> | Surface<br>C/N <sup>2</sup> | S <sub>BET</sub> <sup>3</sup><br>(m <sup>2</sup> /g) | V <sub>pore</sub> <sup>4</sup><br>(cm <sup>3</sup> /g) |
|--------|------------------|-----------------------------|--|--|
|        | BCN              | 0.67                        | 0.76   | 12.8   |
| SSCN   | 0.68             | 0.81                        | 48.0   | 0.12   |
| DSCN   | 0.66             | 0.81                        | 42.4   | 0.09   |

<sup>1</sup> Elemental analysis.

<sup>2</sup> XPS spectra.

<sup>3</sup> BET methods.

<sup>4</sup> p/p<sub>0</sub>=0.95.

Table S2. The phase of the products obtained from melamine polymerization with MCM-41 or without MCM-41 at different temperatures.

| Temperature (°C) | Phase <sup>1</sup>                       |                                 |
|------------------|--|---------------------------------|
|                  | Without MCM-41                           | With MCM-41                     |
| 200              | melamine                                 | melamine                        |
| 250              | melamine                                 | melamine                        |
| 300              | melamine                                 | melamine                        |
| 350              | Phase I <sup>2</sup> and II <sup>3</sup> | melem                           |
| 400              | melem                                    | melem                           |
| 450              | melem                                    | melem                           |
| 500              | g-C <sub>3</sub> N <sub>4</sub>          | g-C <sub>3</sub> N <sub>4</sub> |
| 550              | g-C <sub>3</sub> N <sub>4</sub>          | g-C <sub>3</sub> N <sub>4</sub> |

<sup>1</sup> Analysed with XRD.

<sup>2</sup> phase I: lower temperature oligomers.

<sup>3</sup> phase II: higher temperature oligomers[1].

Table S3. Textural properties of the core/shell silica and series of MS-x silica.

| Sample            | $S_{\text{BET}}$ ( $\text{m}^2/\text{g}$ ) | $V_{\text{pore}}$ ( $\text{cm}^3/\text{g}$ ) | Pore size (nm) |
|-------------------|--|--|----------------|
| Core/shell silica | 443.2                                      | 0.33   | 2.9            |
| MS-1              | 1397.5                                     | 1.43   | 3.8            |
| MS-2              | 1032.3                                     | 1.68   | 5.5            |
| MS-3              | 923.0                                      | 1.34   | 6.3            |

Table S4. The bandgap energy, valence band and conduction band position of BCN, SSCN, Ag@SSCN and DSCN.

| Sample  | Bandgap Energy (eV) | $E_V$ (eV) | $E_C$ (eV) |
|---------|---------------------|------------|------------|
| BCN     | 2.47                | 1.63       | -0.84      |
| SSCN    | 2.55                | 1.87       | -0.68      |
| Ag@SSCN | 2.29                | 2.10       | -0.19      |
| DSCN    | 2.56                | 2.14       | -0.42      |

Bandgap energy ( $BE$ ) is determined by the Tauc plots (Figure S18). The specific position of valence band ( $E_V$ ) is determined through the XPS-VB spectra (Figure S19). The conduction band position ( $E_C$ ) is calculated by the equation:  $E_C = E_V - BE$ .

Table S5. The comparison of the photocatalytic activity of the tailored g-C<sub>3</sub>N<sub>4</sub>.

| Sample  | HER <sup>1</sup> ( $\mu\text{mol}\cdot\text{h}^{-1}$ ) | Kinetic constant <sup>2</sup> ( $\text{min}^{-1}$ ) |
|---------|--|---|
| BCN     | 4.1  | 0.005   |
| SSCN    | 14.3   | 0.013   |
| Ag@SSCN | 18.6   | /   |
| DSCN    | 27.5   | 0.078   |

<sup>1</sup> Photocatalytic water splitting for hydrogen evolution.

<sup>2</sup> Photodegradation of RhB.

## References

[1] B.V. Lotsch, W. Schnick, New light on an old story: formation of melam during thermal condensation of melamine, *Chemistry*, 13 (2007) 4956-4968.